White paper:
Airfoil Evaluator: Development and validation of a 2D inviscid panel method

J. Saverin MSc

Wind Energy Group: Hermann Foettinger Institute, TU Berlin

Email: Sav_flowsol@outlook.com

July 3, 2015

The Airfoil Evaluator [1] is a free online tool which enables any user the access to an extensive library of airfoil profiles. A collaboration between NOVASCIENTIA [2] and SMARTBLADE [3], this online application allows the user to perform a number of transformations to the profile before then performing an evaluation upon it. This evaluates a number of important physical properties pertinent to the physical performance of the airfoil including camber, thickness and curvature information. It is the intention of the team working on the Airfoil Evaluator to eventually have a fully automated analysis not only of structural but also aerodynamic properties of the airfoil in the evaluation, so that the user has ready-to-use data.

The first step towards this goal is the development of a model to simulate the aerodynamics of the airfoil. For the simple reason of its high accuracy and minimal computational expense, a potential flow model has been chosen here. It is important to note that the following assumptions apply for the developed module:

- Inviscid flow, $\nu = 0$
- Steady flow
- Incompressible flow, $\rho = const.$

1 Theory

The theory here follows closely that used for X-Foil [4]. The assumption of irrotational, inviscid flow (permissible for high Re numbers) allows Laplace's equation to be derived:

$$\nabla^2 \phi = 0 \tag{1}$$

Here the quantity ϕ represents the velocity potential, of the which the gradient represents the velocity field of the fluid, $\nabla\phi = \vec{v}$. By representing the airfoil as a superposition of a continuous vortex sheet $\gamma(s)$ and a continuous source sheet $\sigma(s)$, the streamfunction for the airfoil is given by:

$$\Psi(x,y) = u_\infty y - v_\infty x + \frac{1}{2\pi}\int \gamma(s)\,\log r(s;x,y)\,ds + \frac{1}{2\pi}\int \sigma(s)\theta(s;x,y)\,ds \qquad (2)$$

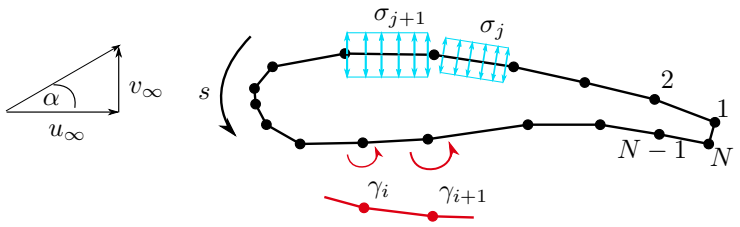

Figure 1: Discretised airfoil surface.

By discretising the boundary of the airfoil into N coordinates, as illustrated in Figure 1, the integral representation above can be broken down into a set of discrete contributions made by N linear panel segments along the contour of the airfoil. The vorticity is taken to vary linearly along each panel and the source strength is assumed to be constant.

1.1 Discretisation of surface

By discretising the surface and considering the potential contribution of each panel, we have a system with $N-1$ panels and equation 2 becomes:

$$\Psi(x,y) = u_\infty y - v_\infty x + \frac{1}{2\pi}\sum_{j=1}^{N-1}\Psi_\sigma(x,y) + \frac{1}{4\pi}\sum_{j=1}^{N-1}\Psi_\gamma(x,y) \qquad (3)$$

where here Ψ_σ and Ψ_γ are values of the integrals of equation 2 evaluated along each panel. For each panel, the values for Ψ_γ can be separated into a portion contributed by node point j, Ψ_γ^-, and a portion contributed by node point $j+1$, Ψ_γ^+. By using the notation $\Psi = \Psi(x,y)$ for brevity, the previous equation becomes:

$$\Psi(x,y) = u_\infty y - v_\infty x + \frac{1}{2\pi}\sum_{j=1}^{N-1}\Psi_\sigma + \frac{1}{4\pi}\sum_{j=1}^{N-1}\Psi_\gamma^+\cdot(\gamma_{j+1}+\gamma_j) + \frac{1}{4\pi}\sum_{j=1}^{N-1}\Psi_\gamma^-\cdot(\gamma_{j+1}-\gamma_j) \qquad (4)$$

1.2 Influence coefficients

By evaluating the integrals of equation 2 along linear panels and under the assumption that the vortex panel strengths vary linearly and the source panel strengths are constant, the potential functions in 4 can be expressed as:

$$\Psi_j^{\gamma+}(x,y) = x_1(\log r_1 - 1) + x_2(1 - \log r_2) + y(\theta_1 - \theta_2)$$
$$\Psi_j^{\gamma-}(x,y) = \frac{1}{x_1 - x_2}\left[(x_1 + x_2)\Psi_j^{\gamma+}(x,y) + r_2^2 \log r_2 - r_1^2 \log r_1 + \frac{1}{2}(x_1^2 - x_2^2)\right]$$
$$\Psi_j^{\sigma}(x,y) = x_2\theta_2 - x_1\theta_2 + y \log \frac{r_1}{r_2}$$

The quantities in the above equation are evaluated in the reference frame of the panel, as illustrated in Figure 2.

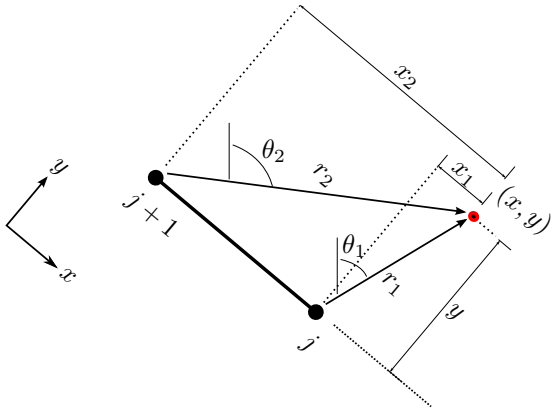

Figure 2: Reference frame of the panel.

1.3 Trailing edge treatment

In the case that the trailing edge is blunt, as illustrated in Figure 3, then an extra condition must be enforced in order to ensure smooth flow from the trailing edge.

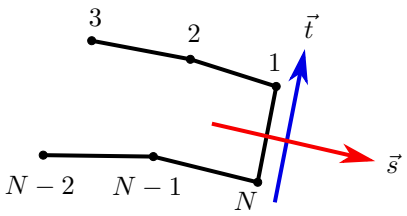

Figure 3: Blunt trailing edge.

A source and vortex panel must be placed across the trailing edge with the following strengths:

$$\sigma_{te} = \frac{1}{2}(\gamma_1 - \gamma_N)|\vec{s} \times \vec{t}| \qquad \gamma_{te} = \frac{1}{2}(\gamma_1 - \gamma_N)|\vec{s} \cdot \vec{t}| \tag{5}$$

This allows us to express equation 4 as:

$$\begin{aligned}\Psi(x,y) =& u_\infty y - v_\infty x + \frac{1}{2\pi}\sum_{j=1}^{N-1}\Psi_\sigma + \frac{1}{4\pi}\sum_{j=1}^{N-1}\Psi_\gamma^+ \cdot (\gamma_{j+1} + \gamma_j) \\ &+ \frac{1}{4\pi}\sum_{j=1}^{N-1}\Psi_\gamma^- \cdot (\gamma_{j+1} - \gamma_j) + \frac{1}{2}(|\vec{s} \times \vec{t}|\Psi_{\sigma,te} + |\vec{s} \cdot \vec{t}|\Psi_{\gamma,te})(\gamma_1 - \gamma_N)\end{aligned} \tag{6}$$

If the trailing edge is sharp, the equations for nodes 1 and N are repeated, which does not allow for a unique solution. This is overcome by specifying that the flow from both sides (approximation to the second derivative) be smooth. This in enforced as: $\gamma_1 - 2\gamma_2 + \gamma_3 = \gamma_N - 2\gamma_{N-1} + \gamma_{N-2}$.

1.4 Composing a linear system

As is well known from potential flow theory, setting the streamfunction to be a constant value gives streamlines of the flow. Taking the surface of the airfoil to be a streamline, along which the streamfunction takes the value Ψ_0 allows equation 2 to be written for each node point (x, y) as:

$$\frac{1}{4\pi}\sum_{j=1}^{N} a_{ij}\,\gamma_j - \Psi_0 = -u_\infty y + v_\infty x - \frac{1}{2\pi}\sum_{j=i}^{N-1} b_{ij}\,\sigma_j \tag{7}$$

Inspection of equation 6 shows that the influence coefficients a_{ij} are given by:

$$a_{ij} = \begin{cases} (\Psi_N^\sigma|\vec{s} \times \vec{t}| + \Psi_N^{\gamma+}|\vec{s} \cdot \vec{t}|) + (\Psi_j^{\gamma+} - \Psi_j^{\gamma-}) & j = 1 \\ (\Psi_{j-1}^{\gamma+} + \Psi_{j-1}^{\gamma-}) + (\Psi_j^{\gamma+} - \Psi_j^{\gamma-}) & j = 2 \cdots N-1 \\ (\Psi_{j-1}^{\gamma+} + \Psi_{j-1}^{\gamma-}) - (\Psi_N^\sigma|\vec{s} \times \vec{t}| + \Psi_N^{\gamma+}|\vec{s} \cdot \vec{t}|) & j = N \end{cases} \tag{8}$$

From N node points we can hence set up N linear equations. There are however $N + 1$ unknowns due to the Ψ_0 term, this is solved by introducing the Kutta condition at the trailing edge:

$$\gamma_1 + \gamma_N = 0 \tag{9}$$

This provides us with a system which can be solved for each of the values of surface vorticity $\gamma_{1,2\cdots N}$. As this particular model solves only for inviscid flow, the values of

source strength on the boundary are taken to be zero $\sigma_i = 0$.

2 Validation

In order to validate the potential flow model, the results have been compared to the well-established code **XFoil** [5] for the following three airfoils:

- NACA0012
- Clark-Y
- NACA 63(3)-618

These are plotted in Figure 4. It shall be elucidated why these particular airfoils were chosen in the separate comparisons. It should be noted for the comparisons which fol-

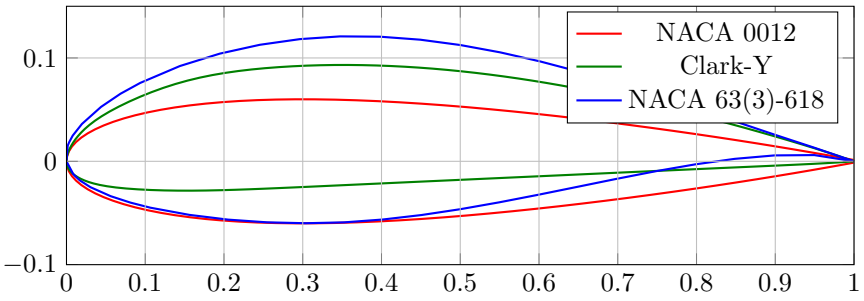

Figure 4: Airfoil profiles for validation.

low that the model developed here is purely inviscid, indicating that the boundary layer surrounding the airfoil is not resolved. The boundary layer is the thin region near the surface of the airfoil where, resulting from the no-slip condition on the wall, shearing forces are very large and the flow is greatly decelerated. This contributes significantly to aerodynamic drag. A further result of flow retardation in the boundary layer is detachment, which leads usually to airfoil stall. As this model takes such effects into account, it cannot be assumed at any point that the results are accurate at angles of attack α where the airfoil is expected to stall. For this reason, the following comparison are limited to regions where the airfoils are not stalled. An attempt has been made to monitor angles of attack which cover sufficiently the attached flow region.

All plots are provided at the end of the document.

NACA 0012

The NACA 0012 is a symmetric profile. As such, it is expected that the $C_p(\alpha, x) = C_p(-\alpha, x)$ and that the suction and pressure sides of the airfoil have an equivalent distribution for $\alpha = 0°$. This can be observed in figure 5. The airfoil has been observed to stall for $|\alpha| \approx 11°$, for which reasons the results have been compared up to $\alpha = 10°$. It is seen that essentially perfect agreement is found between the airfoil evaluator and the inviscid results of XFoil. As can be expected, the disagreement with the inviscid results becomes more pronounced with increasing α, as is seen in figure 6. The NACA 0012 has a blunt trailing edge, it is seen that although the disagreeance with the viscid model is considerable, the agreeance with the inviscid model is again perfect. This demonstrates the Airfoil Evaluator's ability to handle blunt trailing edge airfoils.

Clark-Y

The Clark-Y with 11.7% thickness has been used here, an airfoil commonly used in aviation and well-documented. This airfoil has a sharp trailing edge. It has been observed that the Clark-Y stalls for $\alpha > 14°$ and $\alpha < -6°$. As this profile is asymmetric, the C_P curve is expected to deviate for α positive and negative. This is observed to be the case here, as is illustrated in figures 7 and 8. As was the case previously, perfect agreement is seen between the Airfoil Evaluator and the invsicid XFoil code.

NACA 63(3)-618

The NACA 63(3)-618 is part of a family of airfoils which were designed to maintain laminar flow over their surface at nominal angles of attack, as such it should be expected that the agreement between the inviscid and viscid solutions is relatively good. It is observed that this airfoil stalls for $\alpha > 14°$ and $\alpha < -8°$. As has been observed earlier, excellent agreement is observed between inviscid solutions, however significant divergence is seen from the more realistic viscid solution, this can be seen in figures 9 and 10.

Conclusion

All three airfoils compared have agreed extremely well with the inviscid XFoil analysis of the same airfoils. It can hence be considered that for an inviscid flow module, the Airfoil Evaluator has been validated. It should also however be stated that these results do not correspond to the physical, viscid solutions in many cases and the inclusion of a boundary layer model is necessary for physically reliable solutions. This shall be the focus of future work at NovaScientia and SMARTBLADE.

References

[1] Airfoil Evaluator http://www.airfoilevaluator.com/home.php

[2] Nova Scientia http://www.novascientia.net/

[3] Smartblade. http://www.smart-blade.com/

[4] M. Drela. XFoil: An Analysis and Design System for Low Reynolds Number Airfoils

[5] M. Drela, H. Youngren. http://web.mit.edu/drela/Public/web/xfoil/

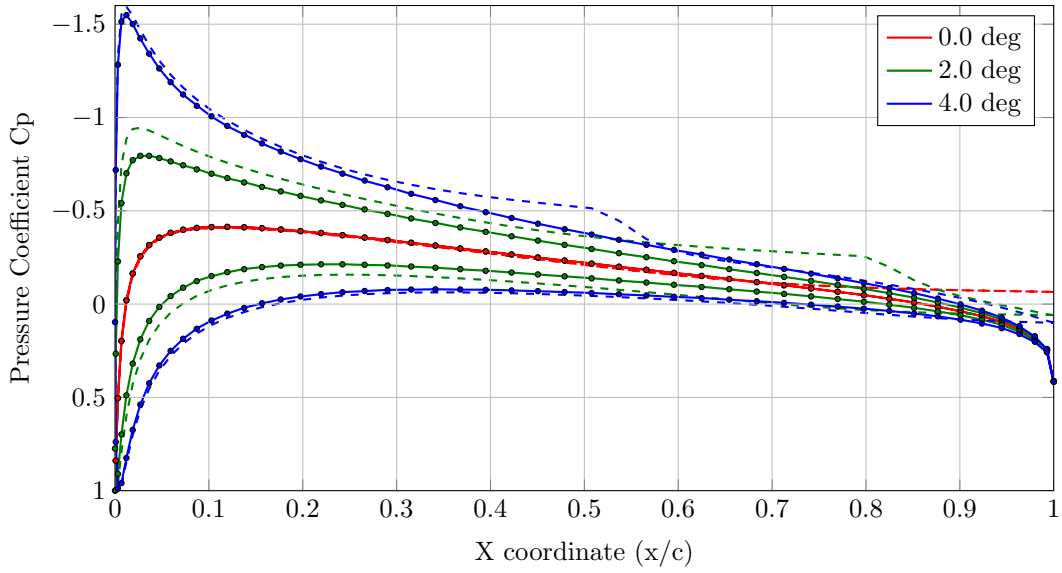

Figure 5: NACA0012 Profile. Line key: Airfoil Evaluator (solid), XFoil inviscid (dotted), XFoil viscid (dashed)

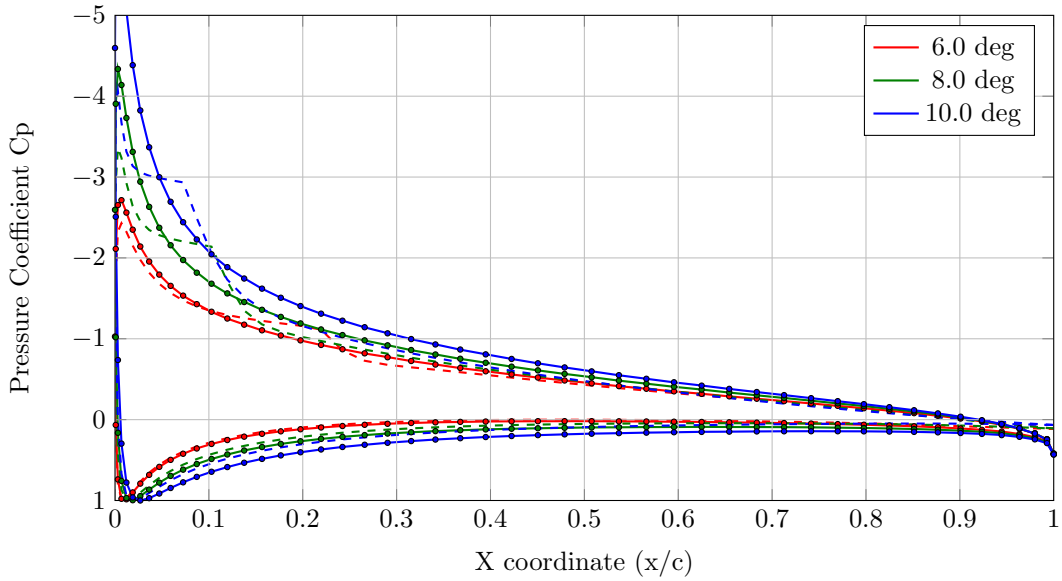

Figure 6: NACA0012 Profile. Line key: Airfoil Evaluator (solid), XFoil inviscid (dotted), XFoil viscid (dashed)

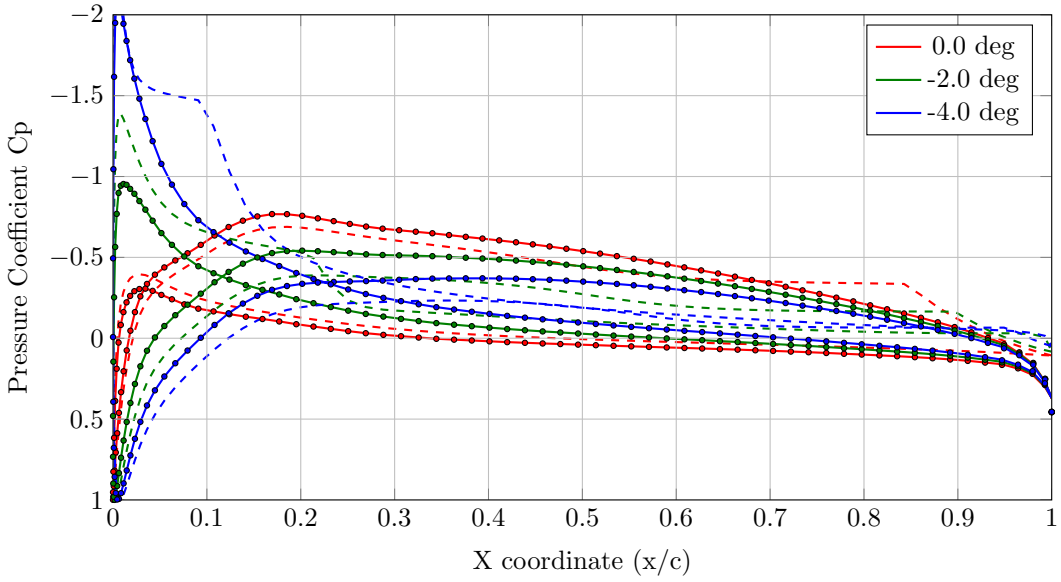

Figure 7: Clark-Y Profile. Line key: Airfoil Evaluator (solid), XFoil inviscid (dotted), XFoil viscid (dashed)

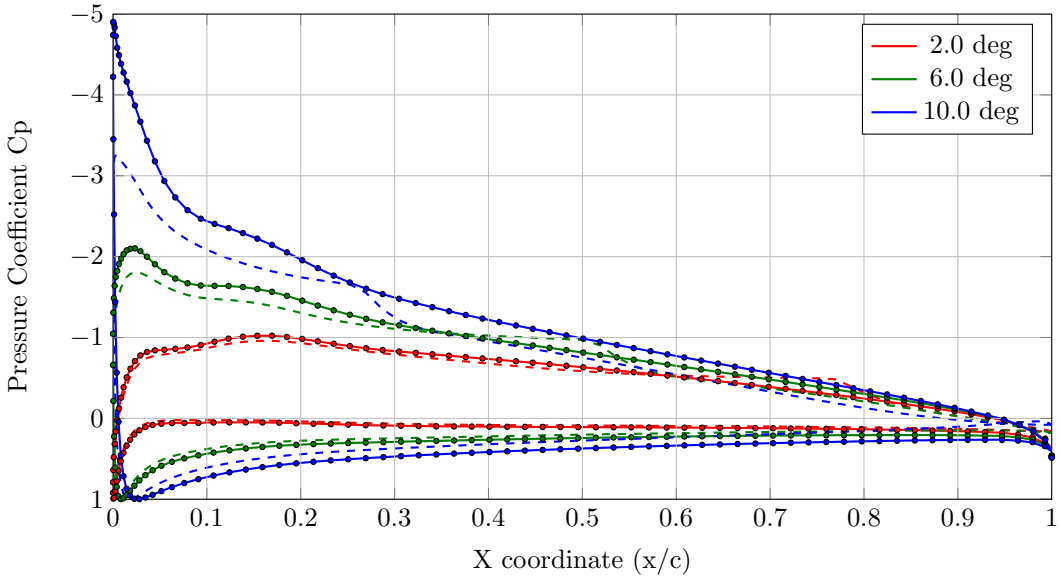

Figure 8: Clark-Y Profile. Line key: Airfoil Evaluator (solid), XFoil inviscid (dotted), XFoil viscid (dashed)

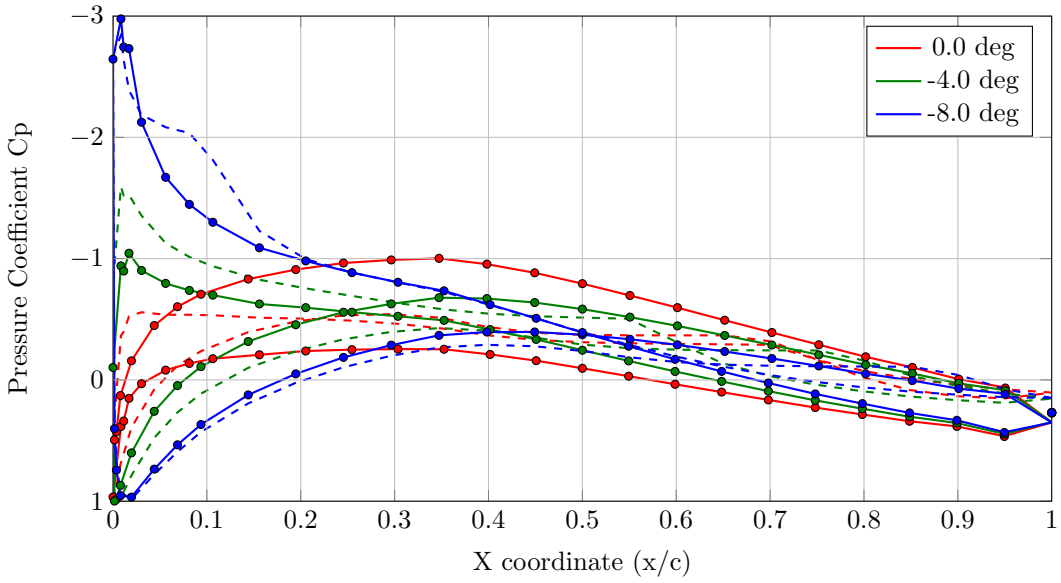

Figure 9: NACA 63(3)-618 Profile. Line key: Airfoil Evaluator (solid), XFoil inviscid (dotted), XFoil viscid (dashed)

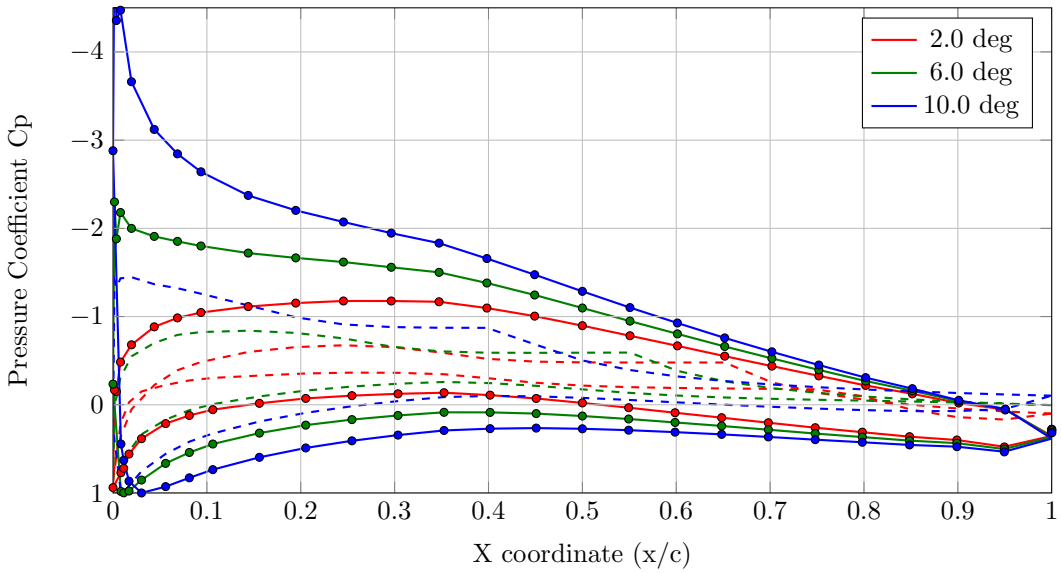

Figure 10: NACA 63(3)-618 Profile. Line key: Airfoil Evaluator (solid), XFoil inviscid (dotted), XFoil viscid (dashed)